Chemical Engineering Journal 162 (2010) 388–395

Contents lists available at ScienceDirect

Chemical Engineering Journal

journal homepage: www.elsevier.com/locate/cej

Experimental study of the nature of gas streaming in deep fluidized beds of Geldart A particles

Shayan Karimipour, Todd Pugsley*

Department of Chemical Engineering, The University of Saskatchewan, 57 Campus Drive, Saskatoon, SK, Canada S7N 5A9

ARTICLE INFO

Article history:
Received 8 March 2010
Received in revised form 19 May 2010
Accepted 20 May 2010

Keywords:
Fluidized bed
Streaming flow
Bed depth
Wavelet analysis

ABSTRACT

The characteristics of gas streaming in a deep gas–solid fluidized bed containing Geldart's Group A powder has been investigated in a 30-cm ID cold flow unit. Four different experimental configurations including forced streaming flow, high and low-velocity jetting and natural streaming flow in deep beds were designed and conducted for bed depths and gas velocities ranging from 0.4 to 1.6 m and from 0.04 to 0.20 m/s, respectively. The range of gas velocities corresponds to 10–50U_{mf} which covers the bubbling fluidization regime. The effect of fines content was studied using two particle size distributions with Sauter mean diameters of 48 and 84 μm, corresponding to 20% and 3% fines content, respectively. Analysis results using autocorrelation and power spectral density (PSD) indicated that the natural streaming closely resembles the forced streaming flow at the wall in which flow of gas is also present in the remaining regions of the distributor. Application of supporting secondary jet injection in addition to the primary gas flow enhanced the fluidization quality to some extent, but was not sufficient to provide fully bubbling fluidization throughout the entire bed. Increasing the primary gas velocity from 10 to 50U_{mf} was found to reduce the effect of supporting jets. It was found that higher fines content improved fluidization. Wavelet analysis of pressure fluctuations showed that in deep fluidized beds, bubbling activity with the typical dominant frequency coexists with the streaming flow, however with a minor contribution to the overall fluidized bed behaviour compared to the prevailing streaming flow. Based on the coexistence of several bubble streams in a bubbling fluidized bed as reported in the literature, Wavelet findings suggested that the streaming flow can be considered to form by increasing the relative importance of one of the available streams of bubbles with increasing bed depth.

1. Introduction

Fluidized bed technology is applied in a range of industrial sectors, including oil refining, coal gasification and combustion, and pharmaceutical manufacture. In certain applications, it is necessary to operate with very deep fluidized beds to control solids and/or gas residence time to achieve reactor performance targets. Recently, it has been revealed that in a sufficiently deep bed of Geldart's Group A particles [1], gas bypassing may occur when the flow rate of the fluidizing gas is increased beyond the minimum fluidization velocity [2–5]. When this phenomenon occurs, the fluidizing gas bypasses the bed in the form of streams of gas, leaving a large fraction of the bed unfluidized or poorly fluidized. Since many industrial fluidized bed processes might work with deep beds, gas streaming is a potential problem that can decrease the efficiency of these chemical and physical fluidized bed processes.

The concept of gas streaming was first reported in the literature by Wells [2]. He studied the effects of fines content (particles smaller than 44 μm), distributor design, anti-static agents, baffles, and bed depth in large scale units with up to 2.5 m diameter and 5 m bed depth. He reported no influence of the various parameters, with the exception of bed depth and baffles. The streaming phenomenon was attributed to gas compression caused by the pressure head of the deep bed over the distributor. The onset of streaming corresponded to an increase in the emulsion suspension density above that at minimum fluidization. The bed then partially defluidized and gas streaming occurred. Karri et al. [3] investigated the formation of streaming flow in a column of 0.3 m inner diameter and 4.9 m height. They found that the standard deviation of pressure drop in a bed exhibiting streaming was much greater than a uniformly fluidized bed. Karri et al. [3] also evaluated the use of baffles and found that two baffles separated vertically by a distance of 0.76 cm eliminated the streaming flow. Issangya et al. [4] performed another study in a 0.9-m diameter and 6.1 m tall test unit. They attributed the larger differential pressure fluctuations measured by certain transducers to the passage of streams closer to that transducer. Issangya et al. [4] also concluded that the max-

* Corresponding author. Tel.: +1 306 966 4761; fax: +1 306 966 5205.
E-mail address: todd.pugsley@usask.ca (T. Pugsley).

1385-8947/$ – see front matter © 2010 Elsevier B.V. All rights reserved.
doi:10.1016/j.cej.2010.05.040

Nomenclature

A1–4	approximate components of the pressure fluctuations time series
ACF	autocorrelation function
D1–4	detail components of the pressure fluctuations time series
PSD	power spectral density (Pa^2/Hz)
t	time (s)
U_0	superficial gas velocity (m/s)
w	wavelet transform operator
x	pressure fluctuations time series (Pa)
X	wavelet transform

Greek letters

ψ	mother wavelet
μ	dilation of the mother wavelet
υ	translation of the mother wavelet

imum in the plot of standard deviation of the pressure fluctuation measured across the entire bed *versus* gas velocity, which has been shown in the literature to be an indication of the transition between the bubbling and turbulent fluidization regimes, is not present for deep beds that are subject to streaming.

Recently, Karimipour and Pugsley [5] have done a systematic study on the streaming flow in a 30-cm ID cold flow unit of FCC particles with two different distributor designs. They discussed the characteristics of the streaming flow based on analysis of the pressure fluctuations time series measured in the fluidized bed at 8 locations from 4 to 150 cm above the gas distributor for bed depths and gas velocities ranging from 0.4 to 1.6 m and from 0.04 to 0.20 m/s, respectively. They also studied the effect of fines content on gas streaming using two particle size distributions with Sauter mean diameters of 48 and 84 μm for each bed depth and gas velocity. They concluded that streaming flow emerges gradually in beds with greater than 1 m depth. Increasing gas velocity and fines content was found to delay the onset of streaming, but were not able to completely eliminate it over the range of velocities examined. They showed that two different distributor designs with much different pressure drops had no measurable effect on the streaming flow.

Wavelet transform is valuable analysis tool for understanding the details of the intrinsic features of fluidized beds. One of the first direct applications of wavelets in fluidized bed research was by He et al. [6]. They used wavelet analysis to decompose the pressure fluctuations time series measured in a fluidized bed with 30 cm diameter and 60 cm bed depth. They argued that the gas jetting at the distributor and formation of small bubbles near the distributor are important sources of Gaussian random noise in the pressure fluctuations. These effects are transmitted upward and reduced gradually by the increase in height and finally superimposed on the larger fluctuations caused by bubble growth and motion. Lu and Li [7] obtained the average peak frequency of different scales of pressure fluctuation time series measured in a 3.3 cm fluidized bed using wavelet decomposition. They found the peak frequency of the scale 4 detail of the wavelet analysis to be equivalent to the bubble frequency obtained from Darton's correlation [8]. Guo et al. [9] decomposed the time series of pressure fluctuations obtained in a 8.2 cm bed with 11.5 cm bed depth operating at high temperatures. By comparison of the detail part of the decomposed signals to the power spectral density (PSD) of the original signal, they concluded that the frequency of peaks in the scale 6 decomposition of detail signal is equal to the major frequency obtained from the PSD plot, thus each peak represents a bubble passing through the pressure probe. Zhao and Yang [10] used wavelets to decompose the pressure time series measured in a 30 cm bed with 46 cm bed depth into several components or "levels". They classified the different levels as micro-, meso- and macro-scales based on the Hurst exponent calculated at each level. Ellis et al. [11,12] studied the effect of probe scale on the voidage data measured by optical probes using wavelets. They showed that the probe size affects the scale of the detected voidage fluctuations in a way that smaller probes reflect small-scale fluctuation, while a larger probe reveals meso-scale fluctuations caused mostly by bubble motion [12]. Sasic et al. [13] extracted and analyzed the time series representing single bubbles, exploding bubbles and pressure waves from the original pressure fluctuations time series using wavelets. These phenomena were identified as distinct local maxima in the energy distribution over wavelet scales. Guenther and Breault [14] studied the cluster size and count at various radial and axial positions in a large scale circulating fluidized bed using fiber optic probes. To remove high frequency noise from the voidage time series, they used wavelets to decompose and then reconstruct the time series excluding scales 1 and 2 of detail components. Their results showed that remarkable changes in the cluster size and count occurred when flow conditions changed from one regime to another. They also found that cluster count generally decreased towards the wall and increased towards the center of the riser.

Although the general appearance of the streaming flow has been studied, a more detailed look at the nature and behaviour of the streaming is still absent in the literature. The objective of the present work is to execute a more fundamental investigation of the streaming flow using a comparative analysis of the streaming with other well-defined phenomena in order to further improve the understanding of streaming gained in the previous works by our group and other researchers. Time series analysis and wavelet decomposition of the pressure fluctuations time series will be used. For this purpose, three well-defined configurations of forced streams and jetting have been designed in order to compare their dynamic behaviour with that of normal streaming flow in deep fluidized beds. Pressure fluctuations have been measured and analyzed in all of these configurations for various combinations of bed depth, gas velocity and particle size.

2. Experimental

The fluidized bed unit used in this study was comprised of a cylindrical Plexiglas column with an inner diameter of 30 cm and height of 3.3 m. Details of the experimental setup, instrumentation and the bed particulate material have been reported in the work of our group [5]. In order to fully understand the nature of the streaming flow in the deep bed (referred to here as "normal streaming"), three configurations for the addition of air to the bed were designed and implemented. The first configuration was a double-jet nozzle made of a copper tube with 4 mm inside diameter and mounted vertically upward at a height of 19 cm above the distributor plate. The arrangement of the nozzle can be seen in Fig. 1. The distance between the two jets was equal to 8 cm. Compressed building air was used for gas flow to the nozzle and the flow rate was measured using a rotameter before entering the nozzle system. The jetting experiments were performed at two combined jet gas velocities of 62 (No. 2) and 120 m/s (No. 1). To force the creation of a stream flow at the wall of the fluidized bed column as opposed to "normal streaming", a lateral opening was cut in the distributor at a location near the pressure transducers. The opening area is supported by a flange from below in a way that gas can enter from the wind-box, but particles cannot leak back into the wind-box. This stabilized the stream in the desired region of the bed for the purpose of further analysis. A diagram of this modified distributor is also shown in Fig. 1. The primary fluidization air through the dis-

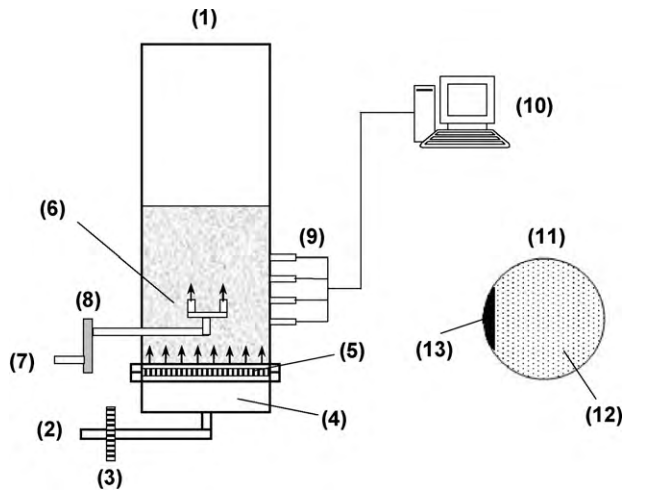

Fig. 1. Schematic diagram of the experimental apparatus, showing the double-jet nozzle and the distributor modified to produce a force streaming flow in the bed: (1) fluidized bed unit, (2) primary air flow from blower, (3) orifice plate, (4) wind-box, (5) distributor, (6) double-jet nozzle, (7) jet air flow from building air, (8) flow meter, (9) pressure transducers, (10) PC and data acquisition system, (11) modified distributor, (12) perforated area, (13) opening area. Arrows in the figure indicate the direction of the air flow.

Table 1
The range of operating conditions studied in this work.

Variable	Range
Bed depth (cm)	40, 160
U_0/U_{mf}	10, 50
Fines content	3%, 20%
Distributor	1 mm holes, square pitch and 0.54% opening; 2 mm holes, square pitch and 2.15% opening
Jet velocity (m/s)	62 (No. 2), 120 (No. 1)

tributor for both natural and imposed streaming was supplied by a 50 hp Kaeser® positive displacement blower. The air flow rate was measured using an orifice plate with a colored water manometer. The ranges of the studied variables are summarized in Table 1.

3. Analysis methods

In our previous study [5] the well-established analysis methods of autocorrelation function, cross correlation function, power spectral density (PSD) and coherency were applied to the fluidized bed pressure fluctuations. In the present study the wavelet decomposition technique has been utilized to decompose the pressure time series into its basic components and extract more detailed information about the streaming phenomenon.

The present theoretical form of the wavelet concept was first proposed by Jean Morlet and the team working under Alex Grossmann in France [15]. The theory of wavelet transformation first appeared in the literature with the work of Grossman and Morlet [16] and was motivated by application to the analysis of seismic data. The main algorithm of wavelet analysis dates back to the work of Mallat [17,18]. Following these efforts in the context of multiresolution signal analysis, Daubechies [19,20] introduced the first highly practical families of orthogonal wavelets.

The wavelet translation of a signal $x(t)$ is defined in terms of projections of $x(t)$ onto a family of functions that are all normalized dilation and translation of a prototype wavelet function $\psi(t)$ such that

$$w\{x(t)\} = X_\nu^\mu = \int_{-\infty}^{\infty} x(t)\psi_\nu^\mu(t)\,dt \tag{4}$$

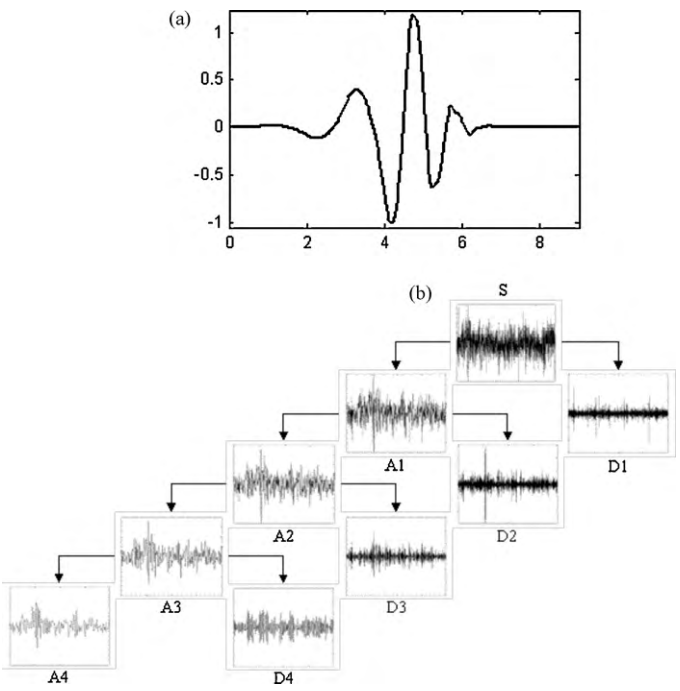

Fig. 2. (a) Daubechies number 5 wavelet ("db5") which has been used in the present work as the mother wavelet. (b) Decomposition of a signal (S) into its components using Wavelet transform.

$$\psi_\nu^\mu(t) = |\mu|^{-1/2}\psi\left(\frac{t-\nu}{\mu}\right) \tag{5}$$

The prototype wavelet, ψ, also called the mother wavelet, possesses some basic properties which are discussed in the wavelet literature [20]. The family of orthogonal wavelets proposed by Daubechies has been broadly used for analysis of time series generated in the fluidized beds in the recent years [9–14]. Daubechies originally provided nine sets of coefficients corresponding to wavelet numbers 2–10 ("db2–db10") [20]. The regularity of wavelets increases with increasing their number. Decomposing the original time series using wavelets with increased regularity provides smoother time series [20]. Considering a trade-off between complexity and regularity, Daubechies number 5 wavelet ("db5") was chosen as the mother wavelet for this study. A plot of this wavelet is provided in Fig. 2a. According to the theory of multi-resolution analysis, an original signal can be decomposed into successive lower resolution components. Fig. 2b demonstrates a schematic diagram of a four level decomposition process. Each level of decomposition contains information associated with a scale. The scale is inversely proportional to the frequency of the Fourier analysis. During the decomposition process, the main body of the signal, with lower frequencies, will be stored as the approximation part (A) and the fluctuating component of the time series as the detail part (D). Continuing the decomposition process makes the approximation part more and more depleted of the high frequency fluctuating components. Therefore, the first detail time series contain the most high frequency fluctuations of the pressure time series.

4. Results and discussions

4.1. Effect of bed depth

Plots of the autocorrelation function and PSD corresponding to a 40 cm bed depth and a gas velocity of $10U_{mf}$ through the distributor are provided in Fig. 3a and b. Pressure fluctuations were measured at 30 cm above the distributor. As Fig. 3a illustrates, all

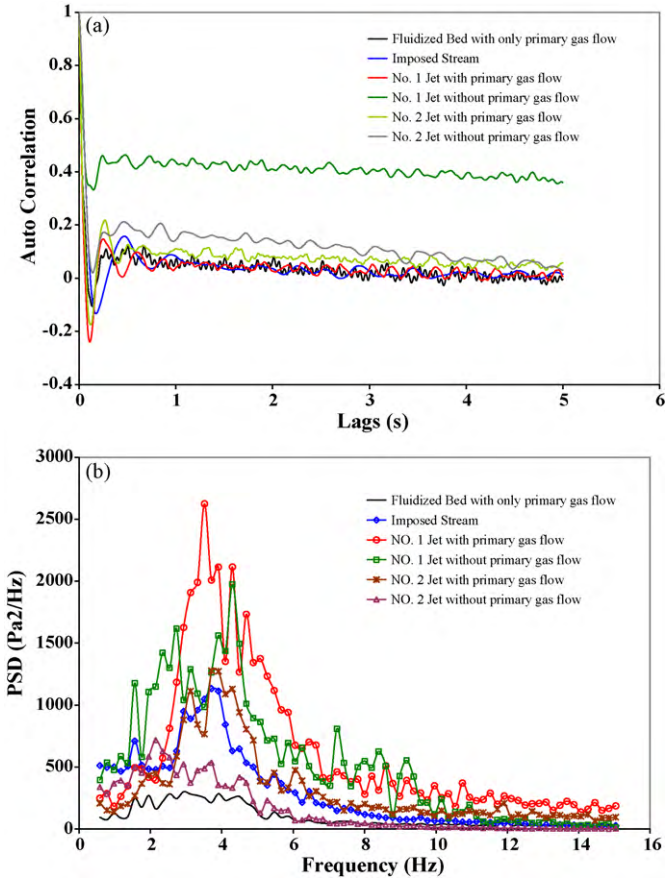

Fig. 3. (a) Autocorrelation and (b) PSD of pressure fluctuations for the different test configurations, 40 cm bed depth, 3% fines content, $U_0 = 10U_{mf}$.

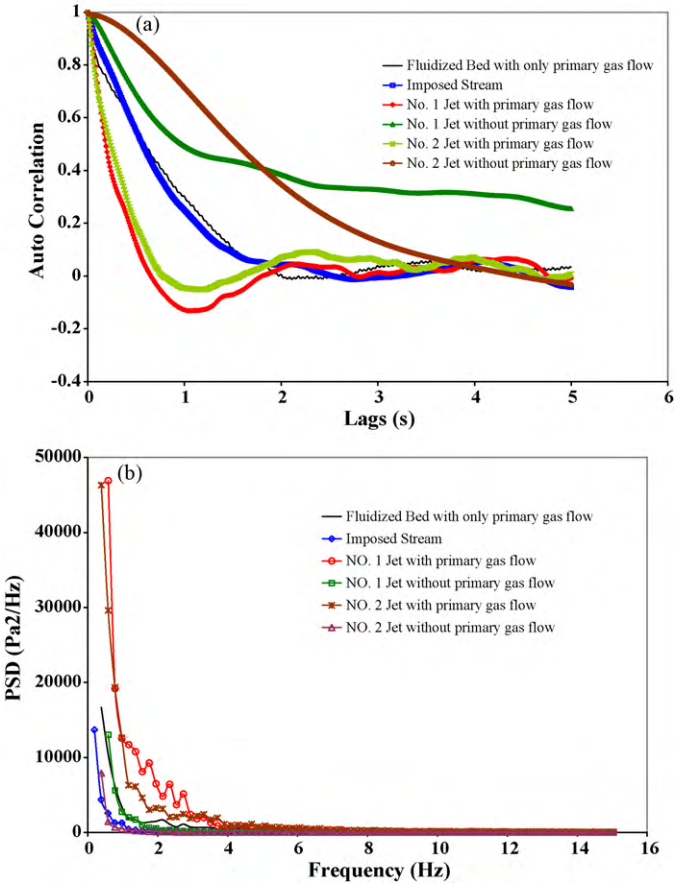

Fig. 4. (a) Autocorrelation and (b) PSD of pressure fluctuations for the different test configurations, 160 cm bed depth, 3% fines content, $U_0 = 10U_{mf}$.

configurations but one exhibit similar periodic oscillations in the autocorrelation function with a rapid initial decrease of correlation or predictability, signifying extensive mixing in the systems. The correlation for the case of high-velocity jet (No. 1 jet) with no primary air flow through the distributor remains higher than other configurations after an initial decrease. This indicates that the gas jet with higher velocity is able to pass through the entire 40 cm bed, with its basic structure remaining intact. Hence, the system exhibits a greater extent of predictability, as evidenced by a higher value of the autocorrelation function. It should be noted that the autocorrelation for this configuration also tends to zero at higher delay times.

The PSD of the various configurations, provided in Fig. 3b, shows that the PSD is spread over a wider frequency domain and the dominant frequency is less distinctive when gas flow only available through the distributor. As can be seen, the presence of a more coherent gas flow in other configurations imposes a clear dominant frequency in the PSD graph. The dominant frequency is 3–4 Hz for all configurations, which is the typical frequency of bubbling beds.

Plots of the autocorrelation function and PSD of the different configurations for a 160 cm bed depth and primary gas velocity of $10U_{mf}$ are provided in Fig. 4a and b. Pressure fluctuations were again measured at a location of 30 cm above the distributor. As can be seen, there are clear differences between these graphs and the previous graphs for the 40 cm bed depth. Especially, the periodic oscillations are absent in the autocorrelation function and the function decays much more slowly. Furthermore, there is a clear shift of dominant frequency towards lower frequencies in the PSD graphs of the fluidized bed with 160 cm bed depth. We have presented these phenomena previously [5] and consider them to be characteristic of non-uniform flow and streaming in deep beds. According to Fig. 4a, the configurations that resulted in similar fluidization for the shallow bed, create three different classes of behaviour in the deep bed. These classes are: jets with primary gas flow; natural and imposed streams; and jets without primary gas flow. As can be seen, there is a gradual change in the autocorrelation function between these groups. The two jet flows without primary gas, show a gradual decrease plus no observable periodic behaviour. Therefore, these configurations represent a clear departure from the normal fluidization in shallow beds discussed above. The two configurations of natural and imposed streaming produce very similar behaviour, illustrating the similarity in hydrodynamic behaviour between these configurations for the 160 cm bed fluidized bed. As can be seen in the figure, adding jet flow to the fluidized bed affects all characteristics of the autocorrelation graph, including a more rapid decrease of the autocorrelation and the return of periodic oscillation. This indicates an improvement of the fluidization quality when jets are implemented in the bed with fluidizing gas already entering through distributor. The PSDs of all configurations in the 160 cm bed (Fig. 4b) all exhibit a shift towards lower frequencies with no clear dominant frequency. The configuration which includes both primary gas flow through the distributor and high-velocity jet again displays a tendency to have some local frequencies, although trivial compared to the general trend towards lower frequencies.

These results for the 160 cm bed depth suggest that the streaming flow most closely resembles a fluidized bed in which a maldistribution of gas on the distributor leads to bypassing of gas through the bed. Streaming cannot be thought of as a pure jetting fluidized bed with no primary gas flow through the distributor

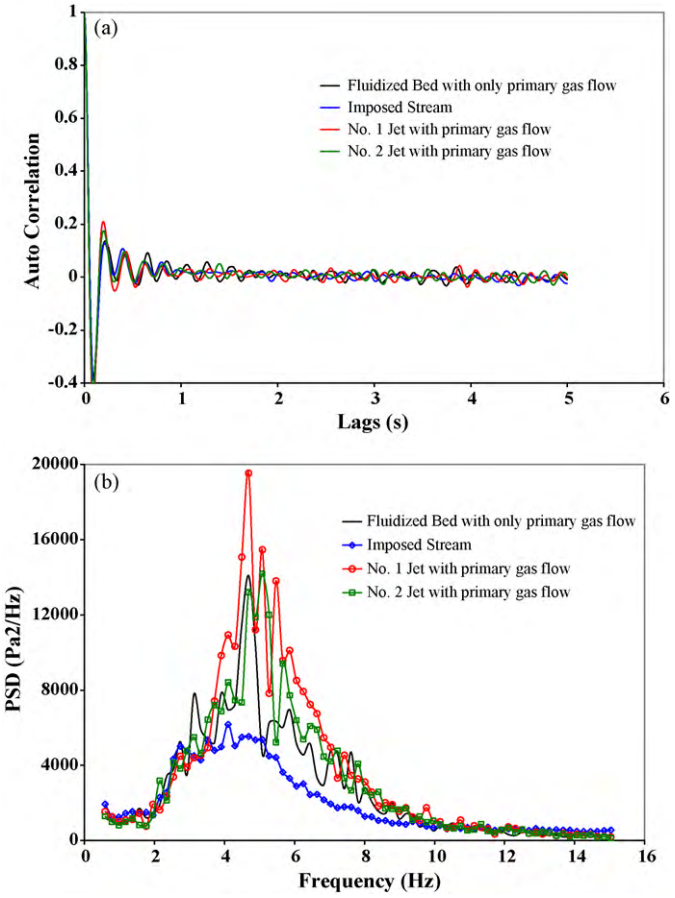

Fig. 5. (a) Autocorrelation and (b) PSD of pressure fluctuations for the different test configurations, 40 cm bed depth, 3% fines content, $U_0 = 50U_{mf}$.

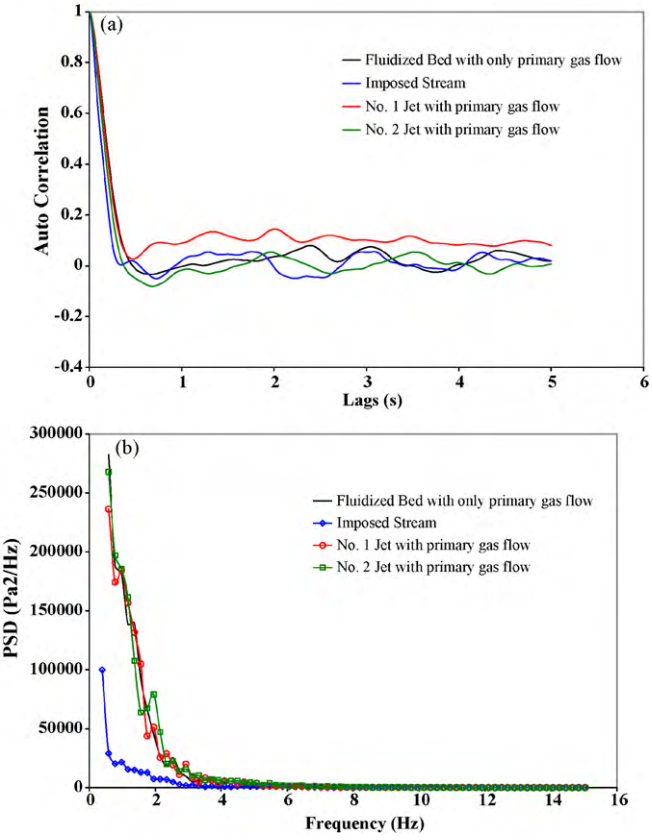

Fig. 6. (a) Autocorrelation and (b) PSD of pressure fluctuations for the different test configurations, 160 cm bed depth, 3% fines content, $U_0 = 50U_{mf}$.

because of both relatively larger size of streams compared to jets (which allows the gas to diffuse into and fluidize other parts of the bed) and availability of the gas entering through the distributor to provide a minor component of gas into the bed cross sectional area.

4.2. Effect of gas velocity

Fig. 5a and b provides the autocorrelation function and PSDs of the pressure fluctuations for the same conditions as Fig. 3a and b, but with a higher primary gas velocity of $50U_{mf}$. The two configurations of jets without primary gas flow (which are evidently not affected by the primary gas flow) are not shown in these figures. Comparing Figs. 3a and 5a illustrates that increasing the primary gas velocity has a minor effect on the fluidized bed behaviour. Furthermore, a slight increase of dominant frequency by about 2 Hz with increasing gas velocity from 10 to 50 times the minimum fluidization velocity can also be observed by comparing Figs. 3b and 5b. There is a general agreement on the fact of increasing the dominant frequency with increasing superficial velocity in the literature [21–23]. Fan et al. [22] measured the bubble rise velocities in several fluidization regimes, including bubbling, slugging, and turbulent fluidization. They showed that for the bubbling regime both the dominant frequency and the bubble rise velocity increased with increasing superficial velocity. Therefore, the increase of dominant frequency observed here can be attributed to the formation of more, faster-rising bubbles with increasing gas velocity.

Fig. 6a and b provides the autocorrelation and PSD of the pressure fluctuations in the 160 cm bed at the primary gas velocity of $50U_{mf}$. In this case, a more prominent effect of gas velocity on the behaviour of the fluidized bed can be seen by comparing Figs. 4a and 6a. As Fig. 6a illustrates, the rate of decrease of correlation and the amplitude of the periodicity are greater at $50U_{mf}$. This is indicative of improved mixing in the bed at the higher gas velocity. However, as the PSD graph of Fig. 6b shows, the frequency domain does not show a significant change compared to Fig. 4b. It can be concluded that although increasing the gas velocity leads to slight improvement in mixing, it is still not able to provide normal bubbling with bubble frequencies in the typical 3–4 Hz range for fluidized beds. Fig. 6b also signifies that at high primary gas velocities through distributor, the PSD graph of jetting and non-jetting configurations approach each other and the effect of jets for enhancing the fluidization becomes negligible.

4.3. Effect of particle size distribution (fines content)

Fig. 7a and b provides the autocorrelation function of the pressure fluctuations corresponding to 20% fines content, a primary gas velocity of $50U_{mf}$ and bed depths of 40 and 160 cm. The pressure measurement for imposed stream was not available for fine FCC experiments. Comparison of Figs. 3a and 7a illustrates that fluidized beds with 3% and 20% fines content exhibit very similar behaviour in the case of 40 cm bed depth. The rate of decline of autocorrelation is somewhat more for the case 20% fines content which can be related to the tendency to form channeling flow in fluidized beds of fine particles. A comparison between Figs. 4a and 7b reveals that particle size has a visible influence on the characteristics of different flow regimes studied here in the 160 cm deep bed. As can be seen the appearance of the graphs mostly resemble Figs. 3a and 7a of 40 cm bed depth, thus, showing the tendency of the system towards a normal bubbling fluidized bed. The two cases

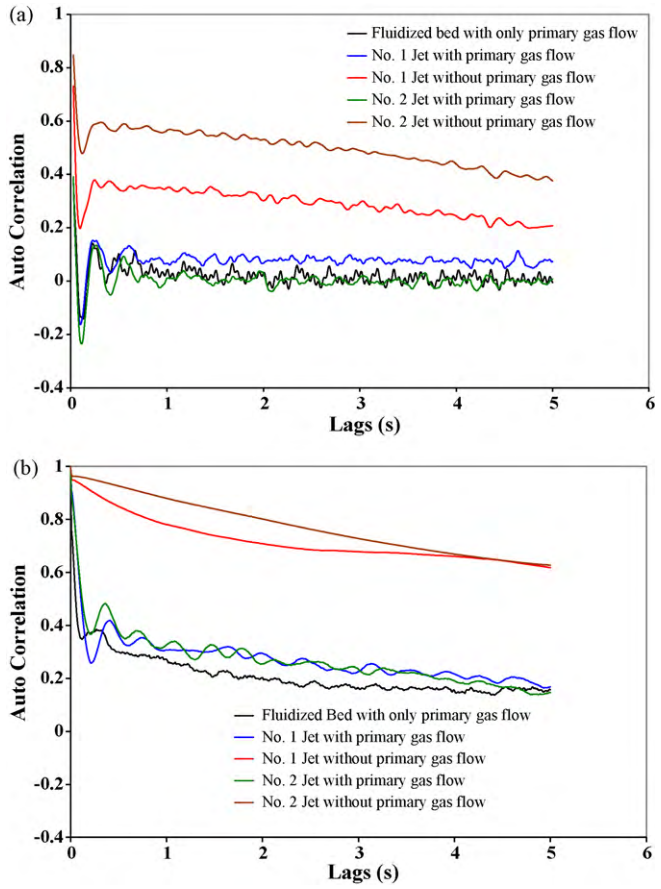

Fig. 7. The autocorrelation function of pressure fluctuations for the different test configurations, 20% fines content, $U_0 = 10U_{mf}$, (a) 40 cm bed depth, (b) 160 cm bed depth.

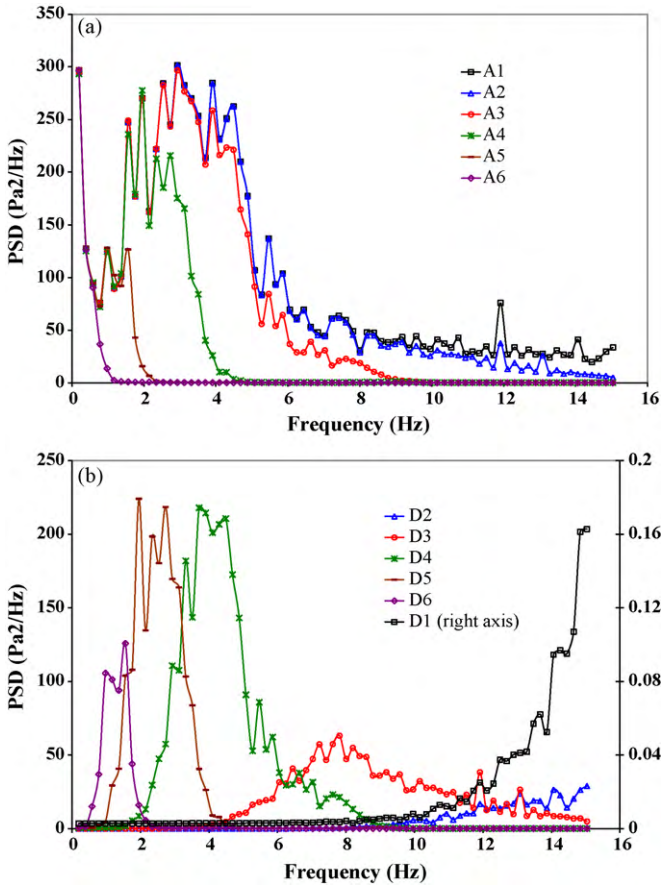

Fig. 8. The PSD of the approximate and detail parts of the pressure fluctuations measured for $U_0 = 10U_{mf}$, 3% fines content in 40 cm bed. (a) Approximate (A). (b) Detail (D).

of jet flows without primary gas flow decline very slowly compared to Fig. 4a of FCC particles with 3% fines content. As mentioned above, this feature can be attributed to the intrinsic characteristics of fines particles to form channels and possible effect of jets to create these phenomena in the bed. The endurance of the pressure fluctuations they cause, and the statistical similarity of the events in the bed at different times might lead to these types of autocorrelation graphs.

4.4. Wavelet decomposition and analysis

The time series of the pressure fluctuations measured using the 3% fines content FCC has been used for wavelet analysis here. For this purpose, the time series is decomposed into 6 levels or scales. Then, the PSD of the resulting approximate and detail parts of the time series have been calculated. The PSD of the approximate and detail parts for 40 cm bed, 160 cm bed, imposed stream and high-velocity jet are provided in Figs. 8–11. As can be seen in Fig. 8a, the shape of the PSD graph and the dominant frequency of the approximate time series remain almost constant at around 3 Hz until scale 3 of the decomposition. This dominant frequency is equal to the dominant frequency of the original pressure fluctuation time series (Fig. 3b) and is related to the bubbling activity in the fluidized bed. Following scale 3, a decrease in the dominant frequency and power occurs. This indicates that by transferring from scale 3 to scale 4 decomposition, a change in the content of the time series occurs that removes the contribution of bubbling activity from the main body of the time series. Studying Fig. 8b shows that the first two detail time series contain very high frequency fluctuations. However, the power of these fluctuations is very low relative to the power of the next detail time series, which indicates their limited contributions in the main pressure time series. The PSD of scale 4 detail time series shows the higher power and a dominant frequency of less than 4 Hz, which is similar to the dominant frequency of the approximate time series of less than scale 3 decomposition. Hence, the contribution of the bubbling activity in the original time series transfers from scale 3 approximate to the scale 4 detail time series by continuing the decomposition. As the figure shows, scale 5 detail presents a dominant frequency of 2 Hz. Since the presence of several bubbling activities with different dominant frequencies has been reported in the previous literature [23], scale 5 detail may be indeed presenting another bubbling activity. After decomposition of scale 4, the dominant frequency of the detail parts shifts towards lower frequencies with lower power in the PSD graph. Therefore, it can be concluded that the dominant frequency of 3 Hz, found for 40 cm fluidized bed, is a superposition of these two bubbling activities.

As Fig. 9a indicates, all the approximate times series for 160 cm bed depth provide similar PSD graphs. Only the contribution of the higher frequencies decreases in the PSD with continuing the decomposition, which is generally considered to be trivial. As Fig. 9b shows, scales 4 and 5 detail time series of the 160 cm bed exhibit dominant frequencies of 4 and 2 Hz, respectively, which is similar to the 40 cm bed depths. However, the relative power of the scale 5 component with 2 Hz frequency increases compared to the scale 4 part with 4 Hz frequency. Furthermore, contrary to the 40 cm bed, the power of scale 6 part which possesses lower dominant frequency, increases compared to the previous scales. This signifies the

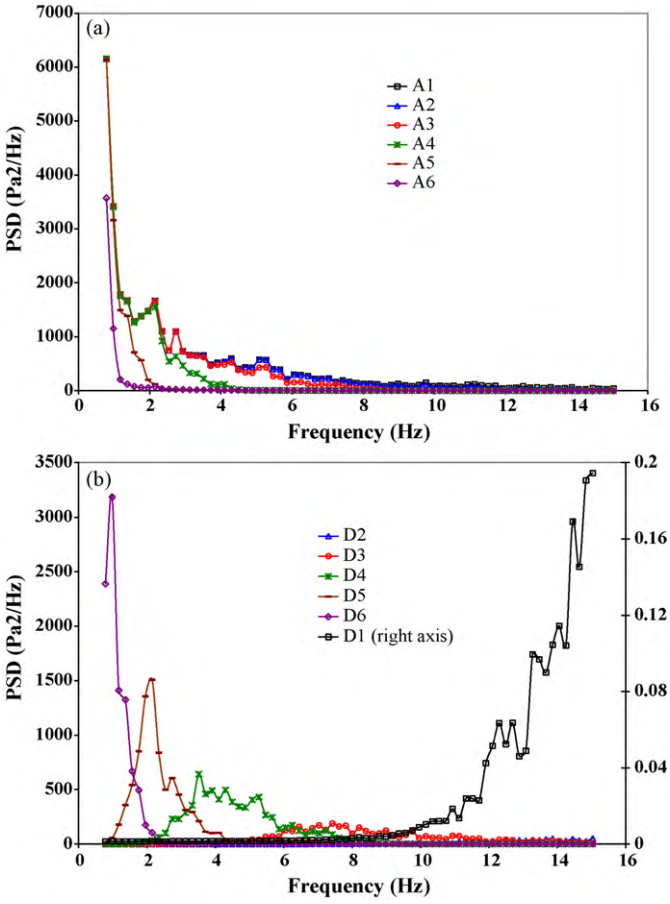

Fig. 9. The PSD of the approximate and detail parts of the pressure fluctuations measured for $U_0 = 10U_{mf}$ and 3% fines FCC in 160 cm bed. (a) Approximate (A). (b) Detail (D).

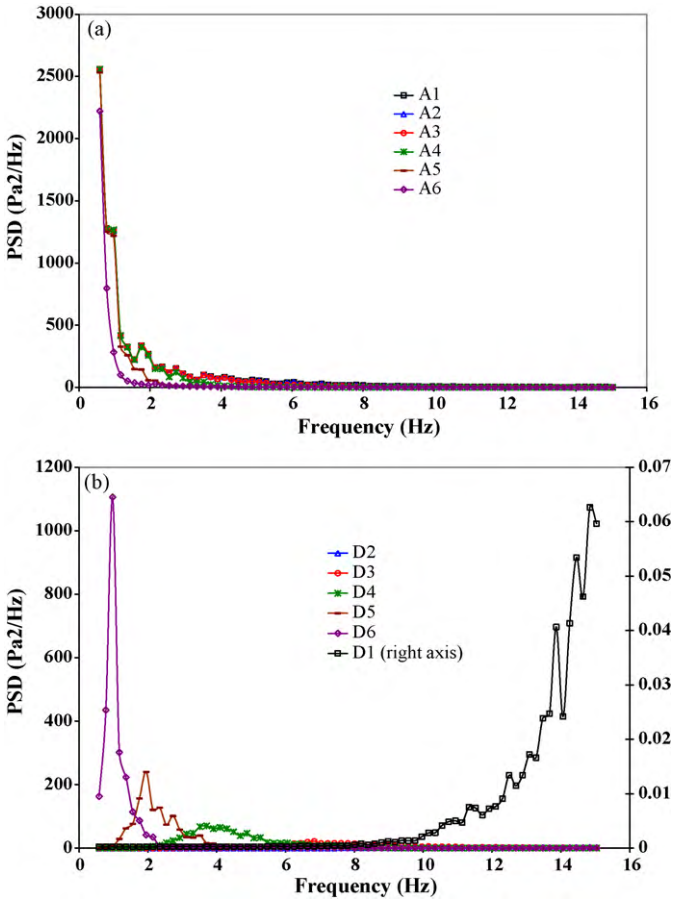

Fig. 10. The PSD of the approximate and detail parts of the pressure fluctuations measured for $U_0 = 10U_{mf}$ and 3% fines FCC in 160 cm bed with imposed stream. (a) Approximate (A). (b) Detail (D).

appearance of other activities with greater influence on the overall fluidized bed hydrodynamics. This can be related to the emergence of streaming flow in the 160 cm fluidized bed. Therefore, it can be postulated that similar bubbling activity that exists in the 40 cm bed fluidized bed is present for 160 cm bed fluidized bed, however, its contribution is much less than the streaming flow that is present at the same time.

Figs. 10 and 11 illustrate the PSD of the approximate and detail parts of the pressure fluctuations for the imposed stream and high-velocity jet configuration in the 160 cm bed fluidized bed. As these figures demonstrate, the power of the higher scale decompositions with lower dominant frequencies gradually increases. The ratio of the power of scale 5 to scale 4 detail compartments, that was found to be the transition point, are calculated as 1, 2.3, 3.6 and 10, respectively, for normal bubbling in the 40 cm bed, natural streaming in the 160 cm deep bed, imposed stream in the 160 cm deep bed and high-velocity jet without primary air flow. These numbers reveal a gradual change of power ratio from a case of shallow fluidized bed containing normal bubbling activity with a uniform distribution of gas towards a packed bed with one internal jet. Therefore, streaming flow can be considered to form by increasing the relative importance of one available stream of bubble activity compared to other activities with increasing the bed depth and suppressing the uniform gas distribution. It should be noted that although fluidized beds with different bed depths apparently have PSD powers with different orders, the calculated values, discussed above, are dimensionless power ratios and thus, are not influenced by absolute values of power.

A thorough review of the literature reveals that these findings can be explained by the observations reported previously by other authors. Rowe and Yacono [24] compared the bubbling fluidization of different particle sizes based on the concept of permeability. The permeability is defined as the ability of gas to diffuse into the bed of particles and is related to the bed voidage. They found that the permeability decreases for deeper fluidized beds. The presence of preferred bubble tracks and channeling has also been reported in the literature by various researchers [24–26]. Furthermore, Matsuno and Rowe [27] have argued that bubbles prefer to rise successively along the preferred paths and increasing the superficial gas velocity increases the number of bubbles, thus their frequency, in a specific path rather than generating new paths. It is probable that some adjacent streams of fast bubbles join each other to form streams of gas in the fluidized bed. Since permeability is expected to be much lower at the bottom of very deep beds, these bubble streams can be stabilized in the bed, especially at the bottom region. Other available bubble streams can gradually join this stream and provide a lower pressure drop passage for the gas flow. Therefore, the streaming would be directly related to lower permeability at the bottom of the deep bed for fluidized beds of small particles. This is in conformity with visual observations reported in our previous work [5] and the findings of this work which indicate that streams form by changing the relative importance of the activities present in the bed with increasing bed depth. Other, less important bubble streams that have not attached to the main stream can also be simultaneously present in the system.

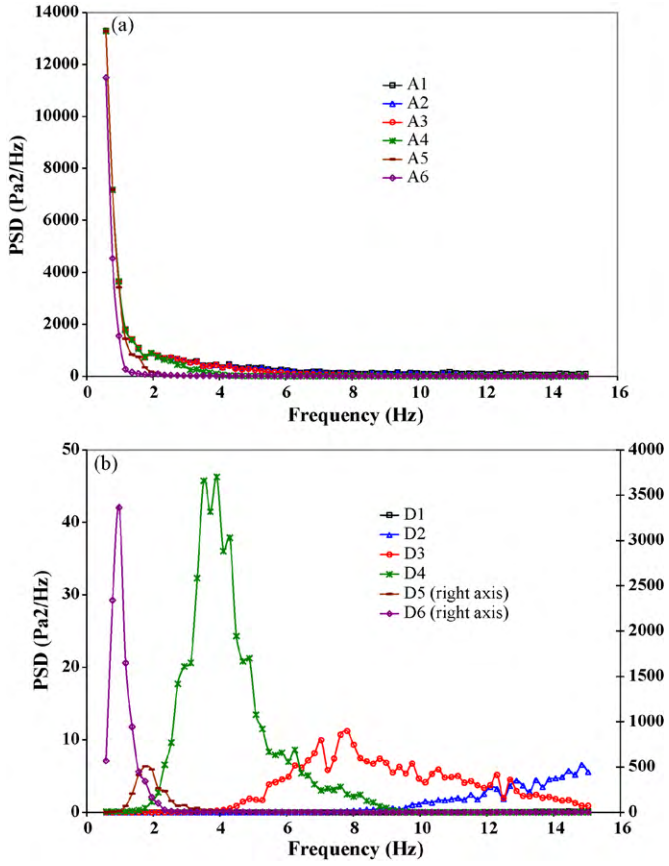

Fig. 11. The PSD of the approximate and detail parts of the pressure fluctuations measured for $U_0 = 10U_{mf}$ and 3% fines FCC in 160 cm bed with NO. 1 jet. (a) Approximate (A). (b) Detail (D).

5. Conclusions

Study of natural streaming flow, forced streaming, and jetting flows revealed that there is no significant difference between the configurations for a fluidized bed with 40 cm bed depth. However, differences emerge by increasing the bed depth to 160 cm. It was found that the natural streaming in a deep fluidized bed closely resembles the case of forced stream in which the gas flow is also present in the remaining regions of the distributor. The jet flows without the primary gas flow could be considered as the cases of severe streaming that might happen in very deep beds with possible formation of completely non-fluidized regions. Application of supporting jets with primary gas flow could enhance the fluidization quality to some extent. Increasing the primary gas velocity from 10 to $50U_{mf}$ was found to reduce the effect of supporting jets. It was also found that finer FCC particles relatively represent better fluidization. Wavelet analysis showed that even in deep fluidized beds that are dominated by the streaming flow, bubbling activity with the same dominant frequency as the shallow bed coexists, although with a minor contribution. These findings suggested that the streaming flow can be considered to form by increasing the relative importance of available stream of bubbles compared to other activities as the bed depth increases.

References

[1] D. Geldart, Types of gas fluidization, Powder Technology 7 (1973) 285–292.
[2] J. Wells, Streaming flow in large scale fluidization, in: Paper presented at the AIChE Annual Meeting, Particle Technology Forum, Reno, Nevada, USA, 2001.
[3] S.B.R. Karri, A.S. Issangya, M. Knowlton, Gas bypassing in deep fluidized beds, in: U. Arena, R. Chirone, M. Miccio, P. Salatino (Eds.), Fluidization XI, May, Ischia (Naples), Italy, 2004.
[4] A. Issangya, T. Knowlton, S.B.R. Karri, Detection of gas bypassing due to jet streaming in deep fluidized beds of group A particles, in: F. Berruti, X. Bi, T. Pugsley (Eds.), Fluidization XII, May, Vancouver, British Columbia, Canada, 2007.
[5] S. Karimipour, T. Pugsley, Study of gas streaming in a deep fluidized bed containing Geldart's group A particles, Chemical Engineering Science 65 (2010) 3508–3517.
[6] Z. He, W. Zhang, K. He, B. Chen, Modeling pressure fluctuations via correlation structure in a gas–solids fluidized bed, AIChE Journal 43 (1997) 1914–1920.
[7] X. Lu, H. Li, Wavelet analysis of pressure fluctuation signals in a bubbling fluidized bed, Chemical Engineering Journal 75 (1999) 113–119.
[8] R.C. Darton, R.D. La Naueza, J.F. Davidson, D. Harrison, Bubble growth due to coalescence in fluidized beds, Chemical Engineering Research and Design 55 (1977) 274–280.
[9] Q. Guo, G. Yue, T. Suda, J. Sato, Flow characteristics in a bubbling fluidized bed at elevated temperature, Chemical Engineering and Processing 42 (2003) 439–447.
[10] G. Zhao, Y. Yang, Multiscale resolution of fluidized-bed pressure fluctuations, AIChE Journal 49 (2003) 869–882.
[11] N. Ellis, L.A. Briens, J.R. Grace, H.T. Bi, C.J. Lim, Characterization of dynamic behaviour in gas–solid turbulent fluidized bed using chaos and wavelet analyses, Chemical Engineering Journal 96 (2003) 105–116.
[12] N. Ellis, H.T. Bi, C.J. Lim, J.R. Grace, Influence of probe scale and analysis method on measured hydrodynamic properties of gas-fluidized beds, Chemical Engineering Science 59 (2004) 1841–1851.
[13] S. Sasic, B. Leckner, F. Johnsson, Time–frequency investigation of different modes of bubble flow in a gas–solid fluidized bed, Chemical Engineering Journal 121 (2006) 27–35.
[14] C. Guenther, R. Breault, Wavelet analysis to characterize cluster dynamics in a circulating fluidized bed, Powder Technology 173 (2007) 163–173.
[15] B.B. Hubbard, The World According to Wavelets: The Story of a Mathematical Technique in the Making, second ed., A.K. Peters, Natick, MA, 1998.
[16] A. Grossman, J. Morlet, Decompositions of hardy functions into square integrable wavelets of constant shape, SIAM Journal of Mathematics 15 (1984) 723–736.
[17] S. Mallat, Multiresolution representation and wavelets, Ph.D. Thesis, University of Pennsylvania, Philadelphia, 1988.
[18] S. Mallat, Multiresolution approximations and Wavelet orthogonal bases of $L^2(R)$, Transactions of American Mathematics Society 315 (1989) 69–87.
[19] I. Daubechies, Ten Lectures on Wavelets, SIAM, Philadelphia, PA, 1992.
[20] I. Daubechies, Orthogonal bases of compactly supported wavelets, Communications of Pure Applied Mathematics 41 (1988) 909–996.
[21] R.C. Lirag, H. Littman, Statistical study of the pressure fluctuations in a fluidized bed, AIChE Journal 67 (1971) 11–22.
[22] L.T. Fan, T.C. Ho, W.P. Walawender, Measurements of the rise velocities of bubbles, slugs, and pressure waves in a gas–solid fluidized bed using pressure fluctuation signals, AIChE Journal 29 (1983) 33–39.
[23] D Falkowski, R.C. Brown, Analysis of pressure fluctuations in fluidized beds, Industrial and Engineering Chemistry Research 43 (2004) 5721–5729.
[24] P.N. Rowe, C.X.R. Yacono, The bubbling behaviour of fine powders when fluidised, Chemical Engineering Science 31 (1976) 1179–1192.
[25] P.N. Rowe, Experimental properties of bubbles, in: J.F. Davidson, D. Harrison (Eds.), Fluidization, Academic Press, 1971.
[26] L.R. Glicksman, W.K. Lord, M. Sakagami, Bubble properties in large-particle fluidized beds, Chemical Engineering Science 42 (1987) 479–491.
[27] R. Matsuno, P.N. Rowe, The distribution of bubbles in a gas fluidised bed, Chemical Engineering Science 25 (1970) 1587–1593.